Modeling the dc superconducting quantum interference device coupled to the multiturn input coil

K. Enpuku and K. Yoshida

Citation: Journal of Applied Physics **69**, 7295 (1991); doi: 10.1063/1.347576
View online: http://dx.doi.org/10.1063/1.347576
View Table of Contents: http://scitation.aip.org/content/aip/journal/jap/69/10?ver=pdfcov
Published by the AIP Publishing

Modeling the dc superconducting quantum interference device coupled to the multiturn input coil

K. Enpuku and K. Yoshida
Department of Electronics, Kyushu University 36, Fukuoka 812, Japan

(Received 19 October 1990; accepted for publication 22 January 1991)

In order to study the effect of a multiturn input coil on superconducting quantum interference device (SQUID) characteristics, the radio frequency (rf) properties of the coupling circuit between the SQUID coil and the input coil are studied. For the measurement of rf properties of the coupling circuit, the so-called expanded model of the coupling circuit using normal metals was adopted, which is shown to be very useful for this purpose. It is shown that the SQUID coil cannot be expressed by a simple inductance when the SQUID coil is coupled to the input coil, i.e., many resonant structures are observed in rf properties of the coupling circuit. It is also shown that the damping resistance is useful in suppressing the resonant structures. Using the experimental results, a circuit model of the SQUID coupled to the multiturn input coil is proposed.

I. INTRODUCTION

Direct current (dc) SQUID (superconducting quantum interference device) operating at helium temperature has been intensively studied. In practical applications, a dc SQUID is usually coupled to an input coil, through which the magnetic flux is transferred to the SQUID coil. The multiturn input coil proposed by Ketchen and Jaycox[1] is an excellent method that ensures the tight coupling between the SQUID coil and the input coil. It has been shown, however, that the multiturn input coil causes parasitic effects.[2-5] The characteristics of the SQUID, such as the current-voltage (I-V) and the voltage-flux (V-Φ) relations, are degraded significantly when the input coil couples to the SQUID, compared to those of the isolated SQUID. Therefore, it is very important to eliminate these parasitic effects for optimum operation of the SQUID.

There have been several experimental studies to improve the SQUID characteristics coupled to the multiturn input coil.[3-5] Damping resistors connected in parallel with the input coil[3] or the SQUID coil[4] have been used to suppress the parasitic effects. A double-flux transformer design has been proposed also to avoid the parasitic effects.[5] However, the previous studies were made to some extent by the empirical approach, since it has not been well understood how the multiturn input coil causes the parasitic effects. Therefore, it is very important to clarify the mechanism causing the parasitic effects for the optimum design of the SQUID.

In clarifying the mechanism causing the parasitic effects, it is necessary to study rf properties of the coupling circuit between the SQUID coil and the input coil, as shown below. When the SQUID is current biased, rf currents are generated from Josephson junctions, whose frequency is given by $f = V_{dc}/\Phi_0$, where V_{dc} is the dc voltage across the junction and Φ_0 is the flux quantum. It can be expected that these rf currents couple to the input coil through the coupling circuit, and cause the parasitic effects on the SQUID characteristics. Therefore, we must study rf properties of the coupling circuit, though only a dc property of the coupling circuit has so far been studied. In the usual case, it is necessary to study the frequency range from dc to a few 10 GHz.

In this paper we develop a model of the SQUID coupled to the multiturn input coil by studying rf properties of the coupling circuit. First, we propose an experimental method to study rf properties of the coupling circuit, which is very useful for this purpose. Using the method, we experimentally clarify rf properties of the coupling circuit. Based on the experimental results, we present a circuit model of the SQUID coupled to the multiturn input coil.

II. RF PROPERTIES OF THE COUPLING CIRCUIT

A. Expanded model

In Fig. 1, the SQUID coupled to the multiturn input coil is shown schematically. We experimentally study rf properties of the coupling circuit between the SQUID coil and the multiturn input coil. In terms of circuit theory, the rf properties the coupling circuit can be described by the impedance Z_{AB} measured from terminals A and B of the SQUID coil shown in Fig. 1. It is, however, very difficult to measure directly the impedance of the circuit due to the small geometric size of the circuit and high operating frequency. Therefore, we adopt the so-called expanded model of the coupling circuit. In this model, the geometric size of each element of the coupling circuit is enlarged by a factor of F, compared to the original circuit. In this case, the frequency range to be studied can be reduced to $1/F$. The enlargement

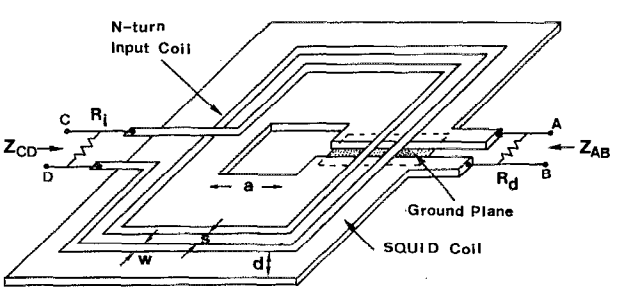

FIG. 1. Schematic figure of the SQUID coupled to the multiturn input coil. The expanded model of the circuit with an expanding factor $F = 500$ is used. Parameters are $N = 33$, $w = 1.5$ mm, $s = 1.5$ mm, $d = 0.5$ mm, and $a = 5$ cm. A ground plane is used to reduce the inductance of the slit in the SQUID coil.

 0021-8979/91/107295-06$03.00

of the geometric size and the reduction of the frequency range make the experiment less difficult.

Furthermore, we propose the use of normal metals instead of superconductors as electrodes of the coupling circuit. The validity of using the normal metal can be shown as follows. When the coupling circuit is made of superconductors, electromagnetic fields penetrate into the superconductor in the region of the London penetration depth λ. However, the value of λ is usually very small compared with the geometric size of the coupling circuit, such as the distance d between the SQUID and input coil shown in Fig. 1. This means that the electromagnetic fields in the superconductor hardly affect the rf properties of the circuit; in other words, rf properties of the coupling circuit are dominated by the electromagnetic fields outside the superconductor. In the case of normal metals, electromagnetic fields penetrate into the region of the skin depth δ. When the value of δ is sufficiently small compared with the geometric size of the circuit, the above discussion holds. Since this condition is easily satisfied as will be shown later, we can study the rf properties of the coupling circuit by using the normal metals.

Based on the above discussions, we adopt the expanded model of the coupling circuit, and use Cu metals as electrodes. The original geometric size is enlarged by a factor of $F = 500$ in the present model. In this case, the frequency to be studied ranges from dc to 40 MHz, corresponding to the frequency range from dc to 20 GHz in the practical SQUID. Parameters of the expanded model shown in Fig. 1 are as follows: width $w = 1.5$ mm, spacing $s = 1.5$ mm, distance $d = 0.5$ mm, number of turns $N = 33$, and the hole size of the SQUID $a = 5$ cm.

The skin depth δ of the Cu metal is given by $\delta = (1/\pi f \sigma \mu_0)^{1/2}$, where σ is the conductivity of Cu metal and μ_0 is the permeability. The value of δ becomes $\delta = 200$ μm at $f = 0.1$ MHz for $\sigma = 5 \times 10^7$ s/m. The smallest geometric size of the circuit is the distance between the SQUID coil and the input coil, which is denoted by $d = 500$ μm in Fig. 1. Since the condition $d \gg \delta$ is satisfied for $f > 0.1$ MHz, we can use the Cu metal instead of superconductors in this case. For a lower frequency $f < 0.1$ MHz, on the other hand, the deviation becomes larger. Therefore, in the following, we study the frequency region $f = 0.1$–40 MHz.

B. Experimental Results

1. Isolated SQUID

First, we study the isolated SQUID, i.e., in the absence of the multiturn input coil. In Fig. 2(a), the impedance Z_{AB} of the SQUID coil is shown, which is measured from terminals A and B in Fig. 1. We can see that the impedance of the SQUID coil can be expressed as $Z_{AB} = j2\pi f L_s$, where $j = \sqrt{-1}$ and L_s is the inductance of the SQUID coil.

In Fig. 2(b), experimental values of L_s are shown when the hole size of the SQUID coil is changed, where the hole size is denoted by a in Fig. 1. As shown in Fig. 2(b), the value of L_s increases linearly with a. Since the relation between L_s and a has been obtained in the case of superconductors, we compare the experimental result with this relation. The relation has been given by[6]

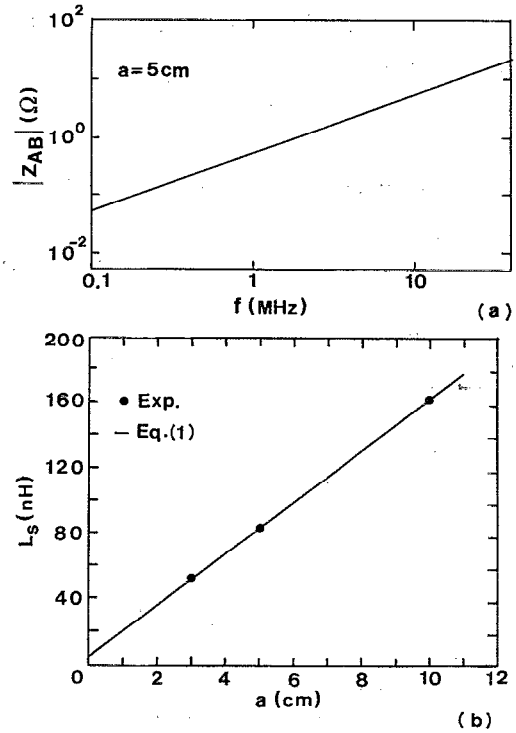

FIG. 2. (a) Impedance of the isolated SQUID coil. The impedance from 0.1 to 40 MHz is measured in the present expanded model, corresponding to the frequency range from 50 MHz to 20 GHz in the practical SQUID. The impedance can be expressed as $Z_{AB} = j\omega L_s$. (b) Relation between the SQUID inductance L_s and the hole size a. The solid line is calculated from Eq. (1) with $L_p = 4$ nH.

$$L_s = 1.25\mu_0 a + L_p, \tag{1}$$

where L_p represents the parastic inductance.

The solid line in Fig. 2(b) is obtained from Eq. (1) with $L_p = 4$ nH. As shown in Fig. 2(b), the experimental results using Cu metals agree well with Eq. (1). This agreement partly confirms the validity of using the Cu metal instead of superconductors.

2. SQUID coupled to the input coil

In the following, we study rf properties of the coupling circuit. In Fig. 3, the impedance Z_{AB} of the SQUID coil is shown when the SQUID coil is coupled to the multiturn input coil. The number of turns of the input coil is $N = 33$, and terminals C and D of the input coil shown in Fig. 1 are opened; resistances R_d and R_i in Fig. 1 are not connected in this case.

Comparing Fig. 3 with the case of the isolated SQUID shown in Fig. 2(a), we can see that the impedance Z_{AB} changes significantly when the input coil couples to the SQUID coil. In the low-frequency region, the impedance Z_{AB} is nearly the same as that of the isolated SQUID. However, in the high-frequency region, peak and dip structures appear in the frequency dependence of Z_{AB}. Furthermore, the values of Z_{AB} outside the peaks and dips are much smaller than those of the isolated SQUID. These results mean that the SQUID coil cannot be represented by a simple inductance when the input coil is coupled to the SQUID coil.

The same result is also observed when the impedance Z_{CD} seen from the input coil is measured; the impedance

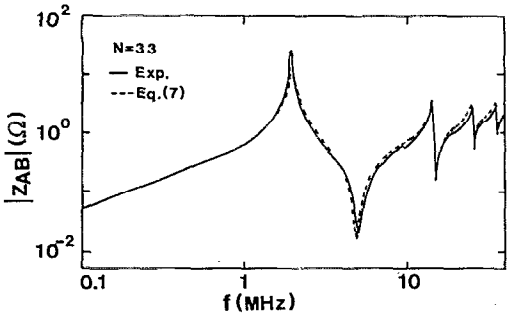

FIG. 3. Effect of the multiturn input coil on the impedance Z_{AB}. Resonant structures are caused by the input coil. The solid line shows the experimental result, and the broken line is calculated from Eq. (7).

Z_{CD} is measured from the terminals C and D in Fig. 1, while the terminals A and B are opened. In Fig. 4, the experimental result is shown. As shown in the figure, the peak and dip structures are observed in the frequency dependence of Z_{CD}.

In the following, we discuss the peak and dip structures shown in Figs. 3 and 4. In order to study the origin of the structure, we number the the peak and the dip of Z_{CD} as $m = 1$–7, as shown in Fig. 4. In Fig. 5, the frequency f_m corresponding to the number m is plotted as a function of m. As shown, the frequency f_m increases almost linearly with the number m.

We can expect that the peak and dip structures are caused by the resonance that occurs between the SQUID coil and the input coil. From Fig. 1, it is expected that the multiturn input coil forms the so-called strip line, while the SQUID coil acts as a ground plane for rf fields. In this case, the standing wave occurs in the strip line when the length of the strip line is equal to m times of the half-wavelength of electromagnetic waves. The condition for the occurrence of the standing wave is given by

$$f_m = (c/2l)(1/\epsilon_r^{1/2})m, \tag{2}$$

where l is the total length of the multiturn input coil, $c = 3\times 10^8$ m/s is the velocity of electromagnetic waves, ϵ_r is the relative dielectric constant, and m is the number of the standing wave.

In Fig. 5, the solid line is obtained from Eq. (2) with $l = 21.2$ m and $\epsilon_r = 1.8$. As shown, experimental results

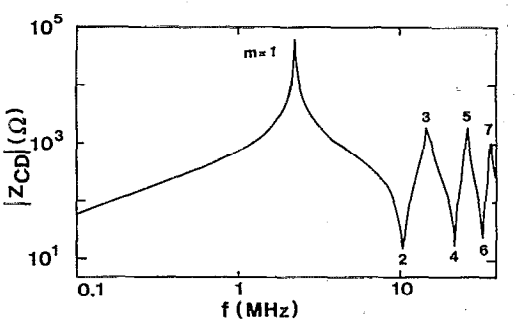

FIG. 4. Resonant structures in the impedance of the input coil Z_{CD}. The peaks and the dips in Z_{CD} are numbered as $m = 1$–7.

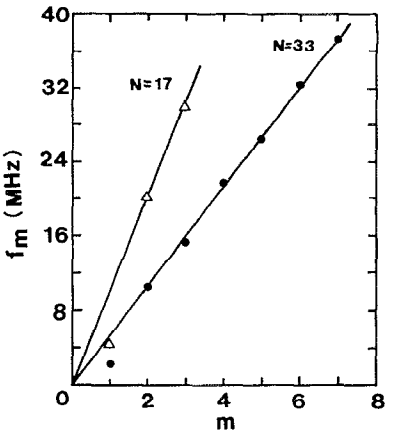

FIG. 5. The relation between the number m and the corresponding frequency f_m shown in Fig. 4. The solid lines show the condition for the occurrence of the standing wave, i.e., Eq. (2).

agree well with Eq. (2) except for $m = 1$; the deviation for the case $m = 1$ will be discussed below. In Fig. 5, we also show experimental results when the total length of the multiturn input coil is changed; the number of turns is $N = 17$ and the total length is $l = 10.9$ m. Good agreement is obtained also in this case. Therefore, it may be said that the peak and dip structures shown in Fig 4 are related to the occurrence of the standing wave; the same result is also obtained for the structures shown in Fig. 3, which will be shown later.

3. Effect of damping resistance

We study the effect of the damping resistance on the rf properties of the coupling circuit. We consider two cases where the damping resistor R_d is connected in parallel with the SQUID coil and the resistance R_i is connected in parallel with the input coil, as shown in Fig. 1. In Fig. 6(a), the impedance Z_{AB} is shown when terminals A and B are shunted with the damping resistor $R_d = 4.5$ Ω. Comparing Fig. 6(a) with Fig. 3, we can see that the peak structure in Z_{AB} can be suppressed when the damping resistor is introduced.

In Fig. 6(b), the impedance Z_{AB} is shown when the terminals C and D of the input coil are shunted by the resistor $R_i = 1$ kΩ. As shown, the peak structure is also suppressed with the resistor R_i. In this case, the value of R_i necessary to reduce the peak structure is much larger than the damping resistor R_d across the SQUID coil, as can be seen from Figs. 6(a) and 6(b).

In Fig. 6(c), we also show the impedance Z_{AB} when the terminals C and D of the input coil are shorted, i.e., $R_i = 0$ Ω. In this case, the peak and dip structures are completely suppressed. The impedance can be expressed as $Z_{AB} = j2\pi f L_{s,\text{eff}}$, where $L_{s,\text{eff}} = 13$ nH is the effective inductance of the SQUID coil. This value is much smaller than that of the isolated SQUID $L_s = 82$ nH.

From the above results, we can say that rf properties of the coupling circuit change considerably in the presence of the input coil. The change of rf properties will cause the so-called parastic effects on SQUID characteristics. Furthermore, the damping resistor improves the rf properties of the coupling circuit; resonant structures in the impedance can be

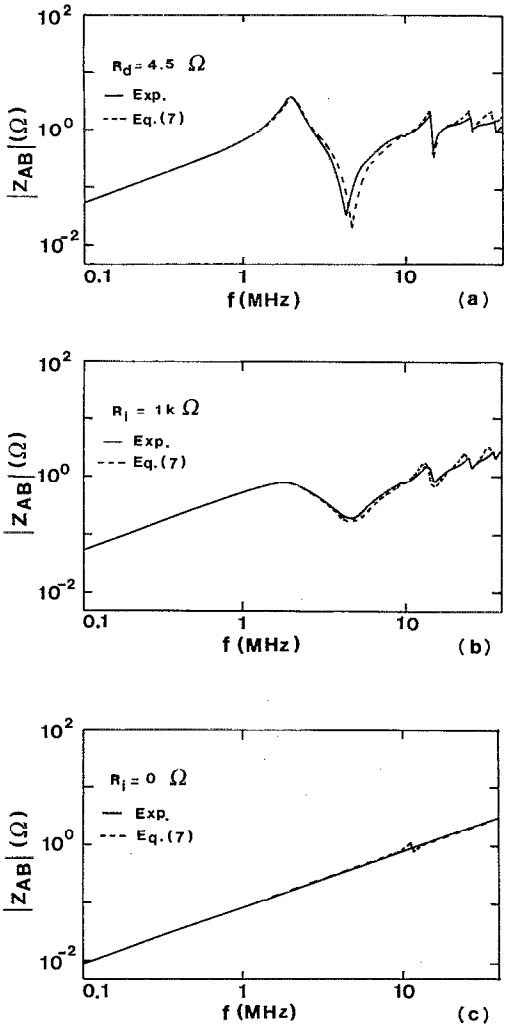

FIG. 6. Effect of the damping resistance on the impedance Z_{AB}: (a) $R_d = 4.5\ \Omega$, (b) $R_i = 1\ \text{k}\Omega$, and (c) $R_i = 0\ \Omega$. The solid lines show experimental results, and the broken lines are calculated from Eq. (7). The resonant structures are suppressed with the damping resistances.

reduced by the damping resistor. This result will explain the previous experimental results[3,4] that SQUID characteristics coupled to the input coil were improved by the damping resistor.

III. MODELING OF THE COUPLING CIRCUIT

A. Equivalent circuit

Using the above experimental results, we develop a model of the coupling circuit between the SQUID coil and the input coil. As mentioned in the previous section, we can expect that the standing wave occurs between the input coil and the SQUID coil. In order to study the standing wave, we consider the simple circuit shown schematically in Fig. 7(a). In Fig. 7(a), we assume that the multiturn input coil acts as a strip line, while the SQUID coil acts as a ground plane. Unlike the usual case, the impedance of the strip line Z_{EF} is measured between the terminals E and F in Fig. 7(a). The expression for Z_{EF} can be obtained as (see Appendix)

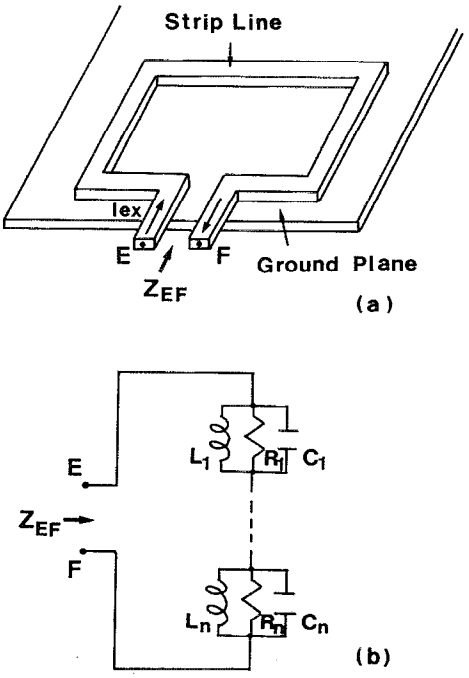

FIG. 7. (a) Schematic figure of the strip line. (b) Equivalent circuit of the strip line. The strip line is expressed by a set of resonant circuits.

$$Z_{EF} = 2jZ_0 \tan(kl/2), \tag{3}$$

where $Z_0 = (L_0/C_0)^{1/2}$ is the characteristic impedance of the strip line, $k = 2\pi f(L_0 C_0)^{1/2}$ is the wave number, L_0 and C_0 are the inductance and the capacitance of the strip line in unit length, respectively, and l is the length of the strip line.

Using the mathematical formula,[7] we can expand Eq. (3) as

$$Z_{EF} = \sum_{n=1} \frac{1}{j\omega C_n + 1/j\omega L_n + 1/R_n}, \tag{4}$$

with

$$C_n = C_0 l/8, \quad L_n = 8L_0 l/\pi^2(2n-1)^2, \tag{5}$$
$$R_n = Q_n(L_n/C_n)^{1/2},$$

where $\omega = 2\pi f$ is the angular frequency, and Q_n is the quality factor of the strip line. In obtaining Eq. (4) from Eq. (3), we add the loss term R_n.

From Eq. (4) we can obtain an equivalent circuit of the strip line as shown in Fig. 7(b). In Fig. 7(b), the strip line is represented by a set of the resonant circuits. The resonant frequency of each resonant circuit gives the frequency at which the standing wave with odd number occurs in the strip line; the number of the standing wave m is given by $m = 2n - 1$.

Using the above result, we propose a circuit model of the SQUID coupled to the multiturn input coil. In Fig. 8, the proposed circuit model is shown. The input coil is represented by a set of the resonant circuits. Each resonant circuit couples to the SQUID coil through a mutual inductance $M_n = \alpha_n(L_n L_s)^{1/2}$, where α_n is the coupling constant. The values of L_n, C_n, and R_n are given in Eq. (5) except for L_1.

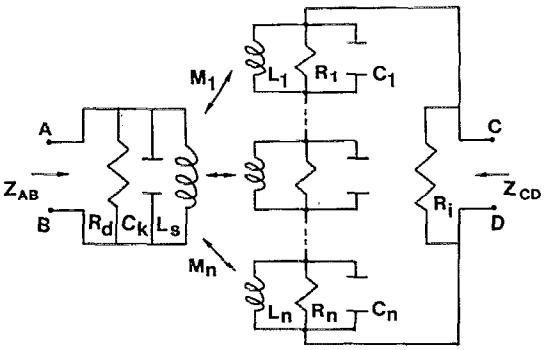

FIG. 8. Proposed circuit model of the SQUID coupled to the input coil. The input coil is expressed by a set of the resonant circuit, and the SQUID is coupled magnetically to each resonant circuit.

The value of L_1 can be obtained as follows. In obtaining Eq. (4), we assume that the SQUID coil acts as a simple ground plane. In the practical SQUID, however, the hole exists in the SQUID coil, as shown in Fig. 1. Therefore, we must take into account that the SQUID coil and the input coil couples magnetically through the hole; it is well known that the magnetic coupling through the hole dominates the dc property of the coupling circuit. In order to include this coupling, the value of L_1 should be changed to

$$L_1 = N^2(L_s - L_p) + 8L_0 l/\pi^2, \tag{6}$$

where $L_s - L_p$ is the inductance of the hole of the SQUID as shown in Eq. (1), and the term $N^2(L_s - L_p)$ represents the magnetic coupling through the hole.

It must be noted that the inductance of the input coil L_i is given by $L_i = \Sigma L_n$ when the frequency $f = 0$, as can be seen from Fig. 8. From Eqs. (5) and (6), we can obtain the relation $L_i = N^2(L_s - L_p) + L_0 l$, which is consistent with the expression for L_i for the case of $f = 0$.

B. Comparison with experiment

From the equivalent circuit shown in Fig. 8, we can study rf properties of the coupling circuit. In the following, we study the impedance Z_{AB} seen from the terminals A and B in Fig. 8, which becomes important in studying characteristics of the SQUID coupled to the input coil. The impedance Z_{AB} can be given by

$$1/Z_{AB} = j\omega C_k + 1/R_d + 1/Z_{sq}, \tag{7}$$

with

$$Z_{sq} = j\omega L_s\left(1 + \sum_{n=1} \frac{\alpha_n^2[(\omega/\omega_n)^2 - j(\omega/\omega_n)(1/Q_n)]}{1 - (\omega/\omega_n)^2 + j(\omega/\omega_n)(1/Q_n)}\right) - \frac{1}{R_i}\left(\sum_{n=1} \frac{j\omega M_n}{1 - (\omega/\omega_n)^2 + j(\omega/\omega_n)(1/Q_n)}\right)^2 \times\left(1 + \frac{1}{R_i}\sum_{n=1} \frac{j\omega L_n}{1 - (\omega/\omega_n)^2 + j(\omega/\omega_n)(1/Q_n)}\right)^{-1}, \tag{8}$$

where $\omega_n = (L_n C_n)^{-1/2}$ is the resonant frequency of the resonant circuit.

In the following, we compare Eqs. (7) and (8) with experimental results obtained in the previous section. In the calculation, parameters in Eq. (8) are chosen as follows. First, the number of the resonant circuit shown in Fig. 8 is set to $n = 4$; note that the value of n is equal to the number of the peaks in Z_{AB} and Z_{CD} shown in Figs. 3 and 4. The resonant frequencies f_n are obtained from the experimental result shown in Fig. 3 as $f_1 = 1.98$ MHz, $f_2 = 13.8$ MHz, $f_3 = 24.7$ MHz, and $f_4 = 34.7$ MHz. Next, the quality factor Q_n is determined from the peak value of Z_{CD} at $f = f_n$ shown in Fig. 4 through the relations $Z_{CD} = R_n$ at $f = f_n$ and $Q_n = R_n/\omega_n L_n$. The values $Q_n = 30$ are estimated; in the practical SQUID using superconductors, the value of Q_n is larger than this value since the loss in Cu metals is included in Q_n in the present case. The coupling efficiency α_n is determined from the peak value of Z_{AB} shown in Fig. 3 through the relation $Z_{AB} = \omega_n L_s \alpha_n^2 Q_n$ in the absence of R_d and R_i; the values $\alpha_1 = 0.91$, $\alpha_2 = 0.14$, $\alpha_3 = 0.09$, and $\alpha_4 = 0.08$ are obtained. The inductance L_n and the capacitance C_n are estimated from Eqs. (5) and (6) as $L_1 = 92.7\,\mu$H, $L_2 = 0.8\,\mu$H, $L_3 = 0.29\,\mu$H, $L_4 = 0.15\,\mu$H, and $C_n = 120$ pF. Finally, the capacitance C_k of the SQUID coil is assumed to be the same order as C_n, i.e., we tentatively assume $C_k = 120$ pF; in the present case, the value of C_k hardly affects the calculated results of Eq. (7) shown below.

In Fig. 3, the impedance Z_{AB} in the absence of the damping resistors R_d and R_i is shown. The solid line is the experimental result, and the broken line is calculated from Eq. (7). As shown in Fig. 3, the present circuit model explains well the rf properties of the coupling circuit between the SQUID coil and the multiturn input coil.

In Figs. 6(a)–6(c), the effect of the damping resistance on the impedance Z_{AB} is shown. The broken lines in Figs. 6(a)–6(c) are calculated from Eq. (7) for $R_d = 4.5\ \Omega$, $R_i = 1$ kΩ, and $R_i = 0\ \Omega$, respectively. The calculated results explain well the experimental results.

From Eq. (7), we can see how the damping resistors R_d and R_i suppress the resonant structure in Z_{AB}. First, we consider the resistance R_d. As shown in Eq. (7), the resonant structure in Z_{AB} arises from Z_{sq}. When the resistance R_d is introduced in parallel with Z_{sq}, the resonances are suppressed as shown in Fig. 6(a) for the case $R_d = 4.5\ \Omega$. Next, we consider the resistance R_i. It can be shown from Eq. (8) that the peak value of Z_{sq} at $\omega = \omega_n$ is given approximately by $Z_{sq} = \omega L_s \alpha_n^2 Q_n[1 - R_n/(R_n + R_i)]$. Therefore, the peak structure in Z_{sq} can be suppressed in the case $R_i \ll R_n$. Since the value of R_n is about a few kΩ in the present case, the value of R_i necessary to suppress the peak structure becomes $R_i = 1$ kΩ, which is much larger than R_d.

As shown above, the circuit model shown in Fig. 8 explains well the experimental results of the impedance Z_{AB}. Since the characteristics of the SQUID are determined by the impedance Z_{AB}, the circuit model is useful to study the characteristics of the SQUID coupled to the input coil. It must be mentioned, however, that theoretical study remains for obtaining the value of each element in Fig. 8; especially, the value of the coupling constant α_n. It must also be mentioned that the model shown in Fig. 8 is not an exact equivalent circuit of the practical coupling circuit; the model is valid only for studying the impedance Z_{AB} and Z_{CD}. For

example, the capacitance between the SQUID coil and the input coil does not explicitly appear in Fig. 8.

IV. CONCLUSION

Rf properties of the coupling circuit between the SQUID coil and the multiturn input coil are studied. The expanded model using the Cu electrode is proposed, which is very useful for this purpose. It is shown that the SQUID coil cannot be expressed by a simple inductance due to the resonant structure that appears in rf properties of the circuit. The resonant structure is caused by the standing wave occurring between the SQUID coil and the input coil. It is also shown that the resonant structures can be suppressed by the damping resistance. These properties of the coupling circuit may explain the so-called parasitic effects of the input coil on the SQUID characteristics. Based on the experimental results, we propose the circuit model of the coupling circuit, which explains well the experimental results. The circuit model will be useful for studying the characteristics of the SQUID coupled to the input coil.

APPENDIX: DERIVATION OF EQ. (3)

Since the length of the strip line shown in Fig. 7(a) is much longer than the wavelength of electromagnetic fields, the strip line must be treated as a distributed circuit. In this case, spatial distributions of the rf current $I(x)$ and the rf voltage $V(x)$ in the strip line are generally given by

$$I(x) = A_1 \exp(jkx) + A_2 \exp(-jkx), \quad \text{(A1)}$$

$$V(x)/Z_0 = -A_1 \exp(jkx) + A_2 \exp(-jkx), \quad \text{(A2)}$$

where $Z_0 = (L_0/C_0)^{1/2}$ is the characteristic impedance of the strip line, $k = 2\pi f(L_0 C_0)^{1/2}$ is the wave number of the electromagnetic waves, L_0 and C_0 are the inductance and the capacitance of the strip line in unit length, respectively. The position x is measured from the terminal E shown in Fig. 7(a); the terminals E and F correspond to $x = 0$ and $x = l$, respectively, where l is the total length of the strip line.

Parameters A_1 and A_2 in Eqs. (A1) and (A2) are determined by the boundary conditions as follows. In the present case, the current I_{ex} is supplied to the strip line from terminals E and F as shown in Fig. 7(a). In this case, the boundary conditions are given by $I(0) = I(l) = I_{ex}$. From these conditions, the parameters A_1 and A_2 can be obtained from Eq. (A1) as

$$A_1 = (I_{ex}/2)[1 - j\tan(kl/2)], \quad \text{(A3)}$$

$$A_2 = (I_{ex}/2)[1 + j\tan(kl/2)]. \quad \text{(A4)}$$

Substituting Eqs. (A3) and (A4) into Eq. (A2), we can obtain the voltages at the terminals E and F shown in Fig. 7(a), i.e., $V_E = V(0)$ and $V_F = V(l)$. Since the voltages V_E and V_F are measured from the ground plane, the voltage V_{EF} across the terminals E and F is given by

$$V_{EF} = V_E - V_F = 2jZ_0 I_{ex} \tan(kl/2). \quad \text{(A5)}$$

Since the impedance Z_{EF} is defined by $Z_{EF} = V_{EF}/I_{ex}$, we can obtain the expression for Z_{EF} as given in Eq. (3).

[1] M. B. Ketchen and J. M. Jaycox, Appl. Phys. Lett. **40**, 736 (1982).
[2] C. Hilbert and J. Clarke, J. Low Temp. Phys. **61**, 237 (1985).
[3] J. Knuutila, A. Ahonen, and C. Tesche, J. Low Temp. Phys. **68**, 269 (1987).
[4] V. Foglietti, W. J. Gallaghar, M. B. Ketchen, A. W. Kleinsasser, R. H. Koch, and R. L. Sandstrom, Appl. Phys. Lett. **55**, 1451 (1989).
[5] J. Knuutila, M. Kajola, H. Seppa, R. Mutikainen, and J. Salmi, J. Low Temp. Phys. **71**, 369 (1988).
[6] J. M. Jaycox and M. B. Ketchen, IEEE Trans. Magn. **MAG-17**, 400 (1981).

[7] We use the mathematical formula $\tan(\pi x/2) = (-4x/\pi) \sum 1/[x^2 - (2n-1)^2]$.